Non-linear site response: a focus of thick sedimentary deposits. Learnings from Japanese strong motion recordings

Pierre-Yves Bard, Ziqian Wang, Hiroshi Kawase, Jikian Sun, Eri Ito, Kenichi Nakano, Boumédiène Derras, Julie Régnier

Non-linear site response: a focus of thick sedimentary deposits. Learnings from Japanese strong motion recordings

P.-Y. Bard [i)], Z. Wang[ii)], J. Sun [iii)], E. Ito [iv)], H. Kawase [v)], K. Nakano [vi)], B. Derras [vii)] and J. Régnier [viii)]

i) Senior scientist, ISTerre, University Grenoble-Alpes, France.
ii) Post-doctoral Researcher, Disaster Prevention Research Institute, Kyoto University, Kyoto / Uji , Japan.
iii) Post-doctoral researcher, Disaster Prevention Research Institute, Kyoto University, Kyoto, Japan
iv) Associate professor, Disaster Prevention Research Institute, Kyoto University, Kyoto, Japan
v) Professor, Disaster Prevention Research Institute, Kyoto University, Kyoto, Japan
vi) Researcher, HAZAMA ANDO CORPORATION, Tsukuba, Japan
vii) Professor, Saida University, & Researcher, RISSAM Laboratory, Tlemcen University, Algeria
viii) Researcher, CEREMA, Sophia-Antipolis / Nice, France

ABSTRACT

This contribution presents a statistical analysis of the non-linear behavior that can be detected on strong motion recordings obtained on thick Japanese sedimentary sites from the KiK-net and K-NET networks, and presents a comparison with other site types, with thinner deposits and/or higher fundamental frequencies. The non-linear effects are quantified by comparing various kinds of site-response characteristics (surface-to-borehole spectral ratios, H/V spectral ratios) for moderate to large motion to their weak motion counterparts. While a non-linear behavior can be detected on thick and thin sites as well, thick sites do not exhibit any peculiar high-frequency reduction. Moreover, from a qualitative viewpoint, the distribution of velocity profiles for sites with very large PGA (above 0.4 g) is similar to the distribution for all strong motion sites in Japan, without any bias towards stiff or shallow sites. The inconsistency of such results with the high frequency decrease predicted by most non-linear simulations warns on the caution to use non-linear degradation curves at large depths, or frequency independent damping.

Keywords: Non-Linear behavior, Thick sites, Degradation curves, K-NET and KiK-net data

1 INTRODUCTION

Numerical simulations of the non-linear response of thick sedimentary deposits give extremely variable results depending on the maximum depth considered for the non-linear behavior of soils. For (non-exceptional) cases where the deep bedrock is hard enough to generate to significant (≥ 2) velocity contrast with the deepest sediments, the application of widely accepted degradation curves to the entire soil column generally leads to a significant reduction of high frequency ground motion even for relatively moderate shaking levels, because deformation levels are high enough to result in significant damping increase over the whole sediment thickness. Nevertheless, as most of these degradation curves have been developed from lab measurements performed under limited confinement pressure, their extrapolation to large depths (exceeding a few hundred meters) can be questioned. The objective of the present study is to compare the observed NL response of thick deposits with a) other sites and b) qualitative predictions.

2 MOTIVATION : THE GRENOBLE EXAMPLE (AMERI ET AL., 2014)

An exercise was performed within the framework of the Sigma Project (Pecker et al., 2017) to investigate the NL response of the 690 m thick sedimentary site of Grenoble corresponding to the location of a nuclear research reactor. For this exercise, as detailed in Ameri et al. (2014), the objective was to estimate the surface motion for a 100 000 year return period with different approaches, from the generic one considering available GMPEs and a VS30 value of 370 m/s, to site-specific ones coupling 1D non-linear site response with Deepsoil (2012) and 3D visco-elastic simulations with Vs and damping values tuned from the 1D approach.

Figure 1a displays the Vs profile, characterized by a gravel layer at shallow depth overlying a thick, rather stiff lacustrine clay deposit with an important velocity gradient, overlying a very hard bedrock (Vs value of 3200 m/s) located at a depth of 690 m. This specific profile exhibits a large velocity contrast at large depth, which automatically results a) in a low fundamental resonance frequency (around 0.3 Hz), and b), for all kinds of wave propagation computations, in a significant strain increase between bedrock and the base of soil column. When considering classical, widely accepted non-linear degradation curves such as Menq (2003) for the top gravel layer, and Darendeli (2001) for the thick clay unit, together with a series of rock input motion with

an average pga around 0.5g (black spectra on Figure 2), the NL effects result in a very significant decrease of surface ground motion compared to the linear case, as also displayed in Figure 2a (surface response spectra) and 2b (amplification factors). Such a decrease is effective over a broad period range, as it starts just above the site fundamental frequency (0.3 Hz / 3 s), is close to a factor of 2 at 1 Hz / 1s, and is approximately constant around 3 for frequencies beyond 2 Hz (periods below 0.5 s). The reason of this large, broad band reduction can be understood by looking at the damping profiles displayed in Figure 1b and Table 1: even though the low strain (elastic) values are around 1%, the strain levels generated over the whole soil column result in much higher damping values, from 3.8 % at the bottom of the clay unit to over 10% at 50 m depth. Considering the ratio between thickness and wavelength, not only the resonance due to vertical interferences can no long exist because waves are too strongly attenuated through their travel up and down in the soil column, but also the primary arrivals are considerably damped during the upward propagation of (large amplitude/large strain) direct waves.

Such predictions are largely controlled by the sensitivity of shear modulus and damping degradation curves to the confining pressure, i.e. to the depth. While such a term does exist in the Darendeli model, there are only very few lab tests providing NL measurements for pressures corresponding to a depth of several hundred meters, and a number of geotechnical engineers prefer not to use them at depths beyond 100 m (A. Pecker and M. Koller, personal communication). As the site response of thick sedimentary deposits is a challenging issue for many areas throughout the world (Mississipi Valley, Japanese coastal plains, Groningen area, among many others), it is important to check whether the available data are supporting such predictions. This is the goal of the next sections, on the basis of the rich set of weak and large amplitude recordings obtained since 1996 by the K-NET and KiKnet stations in Japan.

3 PGA AMPLIFICATION FOR KIKNET BOREHOLE SITES

Increased damping over thick soil columns is expected to produce the largest reduction of ground motion amplification for high frequencies. As PGA is essentially a high frequency ground motion intensity measure, one first check is to investigate the evolution of surface to borehole PGA amplification with increasing ground motion level.

In that aim, we considered in this first exploratory study the KiKnet data set used in Derras et al. (2020) and Régnier et al. (2016), gathering a total of 2927 recordings from 132 different sites, with surface pga exceeding 20 cm/s^2. The major part of this data corresponds to recordings obtained before 2009, augmented by larger amplitude recordings with downhole pga exceeding 50 cm/s^2 obtained in the period 2010-2014. The richness of KiKnet metadata allows to associate to each site different site proxies, including V_{S30} and the fundamental frequency f_{0HV}.

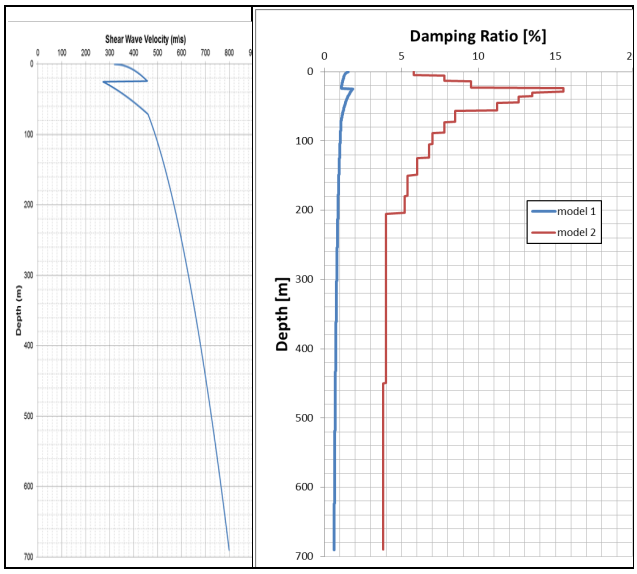

Figure 1: Velocity profile for the Grenoble site (left), and damping profiles (right) corresponding to low strain, elastic values (blue curve) and to the strain levels reached for a 100 000 year / 0.5 g input ground motion (Ameri and Giannakou, 2014)

For each site i and event j, the PGA surface/downhole amplification ratio $AF_{PGA,ij} = PGA_{surf,ij}/PGA_{dwh,ij}$ has been computed. Such a ratio is expected to decrease with increasing loading, for instance with increasing PGA_{surf}, but it is also varying from site to site in relation with the site-specific velocity profile. Therefore, in order to focus only on the evolution (expected reduction) of AF_{pga} with PGA_{surf}, we have normalized this ratio, for each site i, by its low loading value, i.e. the average value of $AF_{pga,i}$ obtained for recordings with a surface pga between 0.1 and 10 cm/s^2 (Régnier et al., 2016).

$$AF_{PGA,ij}^{norm} = AF_{PGA,ij} \,/\, AF_{PGA}^{LIN,i} \quad (1)$$

Examples of such evolutions are shown in Figure 3 for 3 sites, two which exhibit a marked NL behavior with a clear decrease of site amplification with increasing PGA, and one which does not, even though the site has experienced a quite large acceleration (close to 0.7 g). For information the displayed sites are characterized by varying fundamental frequencies and V_{S30}, as listed in Table 2.

Similar evolutions have been analyzed for all possible sites in the above mentioned data base, and could be fitted to an hyperbolic law in the following form for a total of 119 sites with varying site characteristics, from soft to stiff and thick to thin.

$$AF_{PGA,ij}^{norm} = 1./(\,1 + PGA_{surf}^{ij}/PGA_{ref}^{i} \quad (2)$$

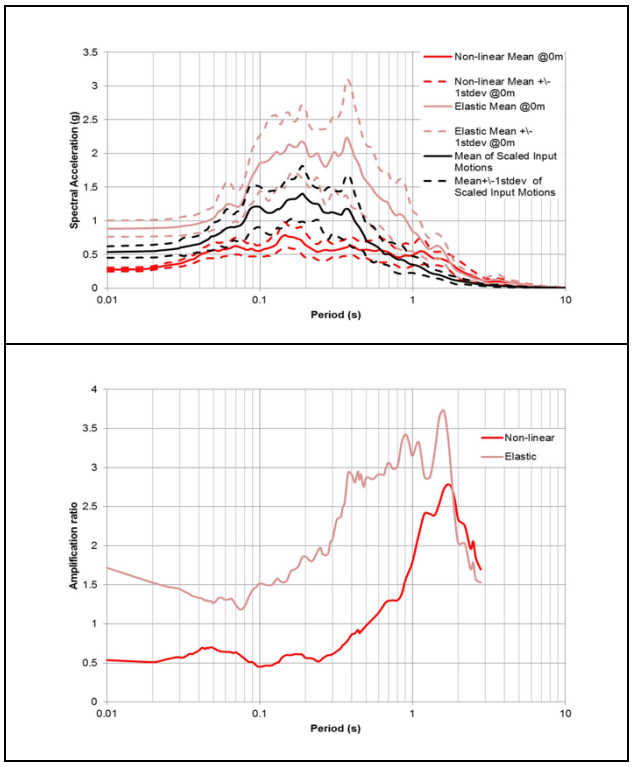

Figure 2: Ground motion Amplification predicted at the Grenoble site in the linear and non-linear cases Top: Range of surface ground motion predicted in the linear (salmon) and non-linear (red) cases for a set of hard rock input accelerograms corresponding to a 100,000 year return period (black). Solid lines correspond to average accelration response spectra, and dashed lines to mean ± 1 standard deviation response spectra. Bottom : Corresponding average surface / hard bedrock amplification factors

Table 1: Damping and peak strain values obtained along the Grenoble soil column for the input rock motion displayed in Figure 2

Depth (m)	Peak Strain from NL Analyses (%)	Damping curve	Damping Ratio (%)	Qs
0-6	0.008	0.25atm M2003	5.8	8.6
6-14	0.022	1atm M2003	7.8	6.4
14-24	0.04	1.5atm M2003	9.5	5.3
24-30	0.3	2atm D2001	15.5	3.2
30-36	0.22	3atm D2001	13.5	3.7
36-45	0.18	3atm D2001	12.6	4.0
45-57	0.15	4atm D2001	11.2	4.5
57-73	0.09	5atm D2001	8.5	5.9
73-89	0.085	6atm D2001	7.8	6.4
89-105	0.075	7atm D2001	7.0	7.1
105-125	0.075	8atm D2001	6.8	7.4
125-150	0.065	10atm D2001	6.0	8.3
150-180	0.06	12atm D2001	5.4	9.3
180-205	0.06	14atm D2001	5.2	9.6
205-450	0.045	16atm D2001	4.0	12.5
450-690	0.04	16atm D2001	3.8	13.2

This equation corresponds to the classical non-linear assumption according which PGA at a given site i cannot exceed a site-specific maximum $PGA_{max,i}$ related to its strength characteristics. From the above equations, this maximum is at least equal to $PGA_{ref,i}$. It is therefore instructive to analyze the sensitivity of these $PGA_{ref,i}$ values to the site characteristics. Figure 4displays the variability of PGAref with the fundamental frequency f0HV (top) and the S-wave velocity proxy V_{S30} (bottom), for all 119 KiKnet sites. the size of the blue symbols is proportional to the quality of the fit, i.e. to the variance reduction provided by the hyperbolic fit (while open symbols correspond to cases where there is no variance reduction, i.e., there is no detectable trend for a decrease of amplification with increasing loading). These figures call for several comments:

i) While almost all soft sites with V_{S30} below 300 m/s do exhibit a clear non-linear trend, there exist a few low f_{0HV} (thus quite thick) sites which do not
ii) Nevertheless, as emphasized in Régnier et al. (2016) and Derras et al. (2020), non-linear behavior can be detected also on stiff sites with V_{S30} beyond 600 m/s, or on high f_{0HV} sites, i.e. for sites with very thin soft layers over stiff bedrock.
iii) A number of sites do not exhibit any clear NL behavior, which results in very high PGA_{ref} values above 5g.
iv) Whenever a non-linear behavior can be detected, PGA_{ref} values do not exhibit any clear trend with either f_{0HV} or V_{S30}. They are varying in the range 200 – 1000 cm/s^2, with an average around 600 cm/s^2 for sites with f_{0HV} below 1 Hz.

A similar analysis has been performed with replacing the loading parameter "PGA_{surf}" by the parameter PGV_{surf}/V_{S30}, which is often considered as a proxy for the peak strain (Idriss, 2011; Chandra et al., 2016; Guéguen et al., 2019), and thus thought preferable to PGA as a measure of the loading intensity for non-linear behavior. A "reference strain proxy" STP_{ref} has thus been derived for the same set of 119 sites, and their sensitivity to f_{0HV} and V_{S30} is displayed in Figure 5. Some peculiar features can also be seen in these plots, some of which are similar to those of Figure 4, and some other different. Only the latter are shortly discussed below.

- The reference strain proxy STP_{ref} is clearly changing with V_{S30} and f_{0HV}: the softer or the thicker the site, the larger is STP_{ref}. The differences reach a factor of 10 (from around 0.01% for V_{S30} around 700 m/s or f_{0HV} around 10 Hz, to 0.1% for V_{S30} below 300 m/s and/or f_{0HV} below 1 Hz.
- This might look in qualitative agreement with the fact that usual NL curves such as Darendeli (2003) consider a dependence on confining pressure (i.e., the depth), as low f_{0HV} sites correspond to thicker soils where NL behavior is expected to occur at larger depth (see Figure 1). Nevertheless, there is major quantitative disagreement since the observed

variability of STP_{ref} exceeds a fac tor 10, while the shear modulus degradation curves are shifted to higher strains by a factor of 2 only from a 25 m depth (2 atm) to a 200 m depth (14 atm).

Similar analyses have been performed for the amplification of a few other scalar round motion intensity measures (PGV, PGV, Arias Intensity, Cumulative Absolute velocity, root mean square acceleration), but cannot be shown here. We prefer to show a few other frequency domain results.

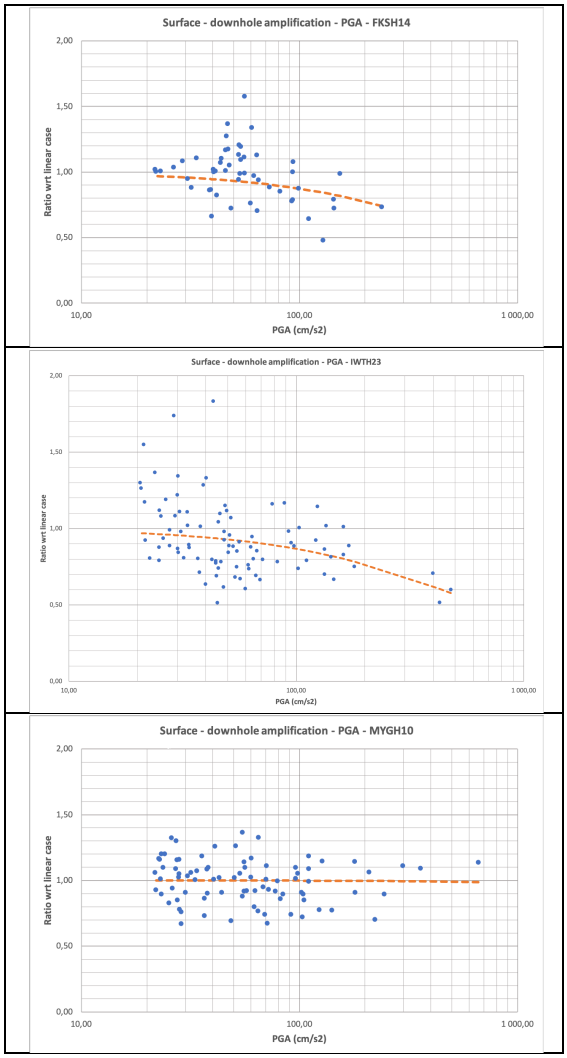

Figure 3: Dependence of normalized amplification with surface PGA for several KiKnet sites. The blue dots are the measurements, the dashed orange line corresponds to the best fitted hyperbolic law.

Table 2: Site proxies and recording characteristics (number, maximum PGA value) for the example KiKnet stations

Site	F_{0HV}	V_{S30}	Number of recordings (pga > 20 cm/s^2)	PGA_{max}
FKSH14	0.22	237	52	238
IWTH23	12.9	923	93	478
MYGH10	0.34	348	85	659

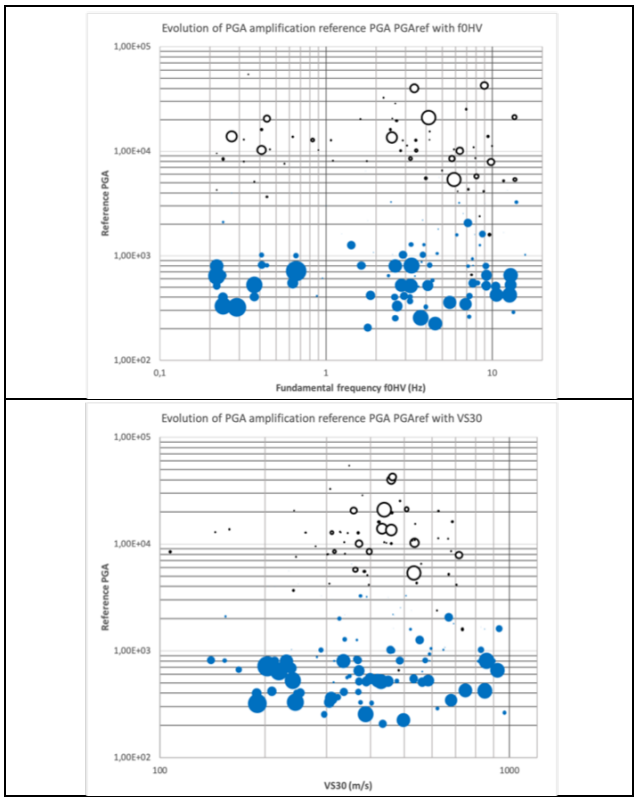

Figure 4: Evolution of "reference acceleration PGAref with fundamental frequency f_{0HV} (top) and V_{S30} (bottom). The size of the blue circles is proportional to the goodness-of-fit to a hyperbolic law, and open circles correspond to sites without any clear non-linear trend (such as MYGH10, see Table 2)

4 FREQUENCY DOMAIN RESPONSE: RSRNL APPROACH

Two approaches have been considered to investigate the evolution of frequency domain site response with the loading level. The first one applies the "RSRNL" approach proposed by Régnier et al. (2013, 2016), consisting in characterizing the non-linear effect by the spectral ratios between the "Borehole transfer function BTF" (i.e., ratio of Fourier acceleration spectrum at surface with respect to the same spectrum at downhole sensor) obtained for a given (strong motion) recording and the "linear BTF", i.e. the same surface / downhole spectral ratio averaged for many weak motion recordings (surface PGA surface between 0.1 and 10 cm/s^2). Our approach is intermediate between the statistical one considered in Régnier et al. (2016a) (average RSRNL for three classes of V_{S30} and/or f_{0HV} and for 3 acceleration thresholds), and the neural network model developed in Derras et al. (2020) allowing to predict RSRNL as a function a loading parameter (PGA, PGV or STP) and one or more site proxies (among which f_{0HV} and V_{S30}).

As we focus here on thick, rather soft sites, we consider 5 f_{0HV} classes (<1, 1-3, 3-5, 5-8 and above 8 Hz) and 10 loading level bins corresponding to an equal number of data. Since the previous section concluded at a non-dependence of PGA_{ref} on f_{0HV} or V_{S30}, we decide

to present here only the results obtained with PGA as the loading intensity measure (rather than STP).The corresponding bins are listed in Table 3. We then computed, for each (f_{0HV}/PGA) bin, the average RSRNL ratio, and plot them as a function of loading level (PGA) for the two extreme f_{0HV} classes in Figure 6.

One can notice that the RSRNL curves for the low frequency (thick) sites do exhibit a high frequency decrease for the large PGA bins (especially the last one, PGA > 232 cm/s^2), but this decrease is significant only for frequencies exceeding 7 Hz, with a maximum reduction of about a factor 2 above 10 Hz. For the Grenoble ground motion predictions shown on Figure 2 (f_{0HV}=0.3 Hz, PGA_{surf} = 0.25 g), the amplification reduction due to NL behavior is around a factor 3 for frequencies exceeding 2 Hz (periods below 0.5 s), and reaches a factor 2 around 1 Hz: such reductions are much higher than those shown in Figure 6 top.

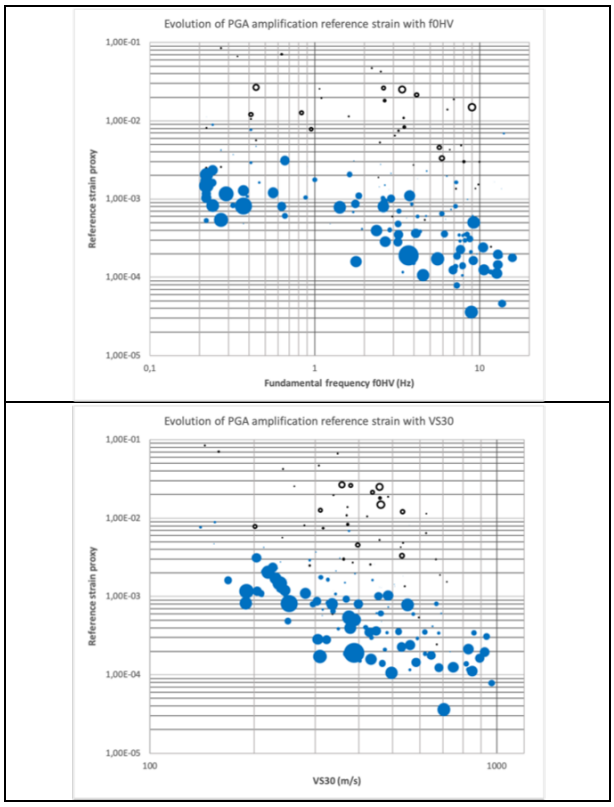

Figure 5: same as Figure 4, evolution of the "reference strain proxy" STP_{ref} with fundamental frequency f_{0HV} (top) and V_{S30} (bottom). The size of the blue circles is proportional to the goodness-of-fit to a hyperbolic law, and open circles correspond to sites without any clear non-linear trend (such as MYGH10, see Figure 3 and Table 2).

From another viewpoint, NL behavior can be clearly identified again on the large PGA bins for high frequency sites: the main difference with low frequency sites is that amplification decrease can be seen only beyond 10 Hz (in which frequency range it is approximately comparable to the statistics for low frequency sites), while there is marked amplification increase between 4 and 8 Hz in relation with the non-linear shift of site fundamental frequency: such an amplification increase is not seen for low frequency sites.

Table 3: PGA ranges for the 10 loading bins

Loading bin	PGA range (cm/s^2)
1	20-33
2	33-45
3	45-70
4	70-81
5	81-92
6	92-105
7	105-124
8	124-156
9	156-232
10	232 - 1500

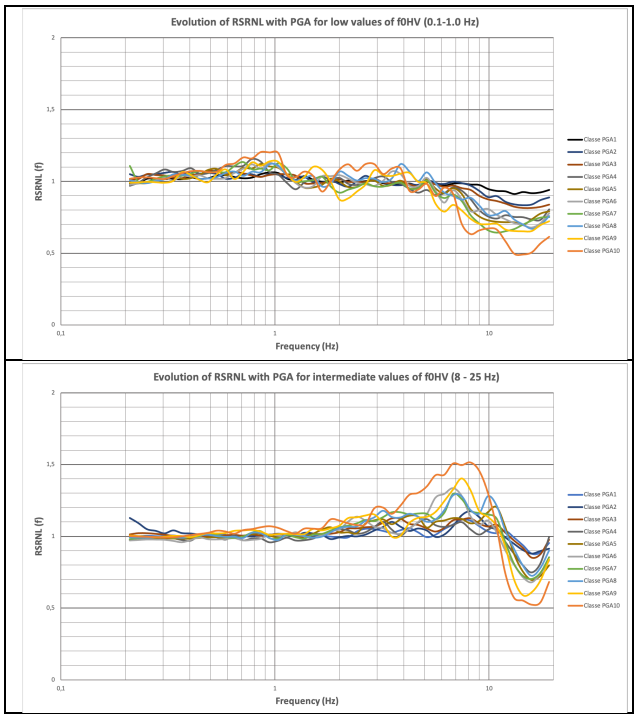

Figure 6:Statistics of RSRNL ratios for different PGA bins (curves with different colors) and the groups of low frequency sites (f0HV < 1 Hz, top) and high frequency sites (> 8 Hz, bottom)

5 FREQUENCY DOMAIN RESPONSE: HVSR APPROACH

DPRI developed an original approach to estimate the NL behavior without needing any reference station: Wang et al. (2021, 2023) compare the H/V ratio $HVSR_E^{NL}(f)$ from the S-wave portion of large amplitude (i.e., PGA ≥ 100 cm/s^2) earthquake recordings to similar ratios $HVSR_E^{L}(f)$ averaged for all weak motion recordings (PGA between 4 and 15 cm/s^2) at the same site, in order to fit two shift parameters α and β according to the following equation

$$HVSR_E^{NL}(f) = HVSR_E^{L}(f * 10^{\alpha}) * 10^{\beta} \quad (3)$$

- α represents a frequency shift on a logarithmic frequency scale. α values are expected to be positive to mimick the low frequency shift due to the NL decrease of shear modulus and wave velocity
- β stands for an amplitude shift : positive values correspond to a NL increase of amplification, while negative values to an amplification decrease

As shown on the example of Figure 7, α and β are fitted through a grid search algorithm minimizing the absolute distance between observed and predicted HV curves, measured over the 0.5 – 20 Hz frequency range with a logarithmic scaling for both frequency and HVSR amplitude values. More details can be found in the two above mentioned papers and in Wang (2022).

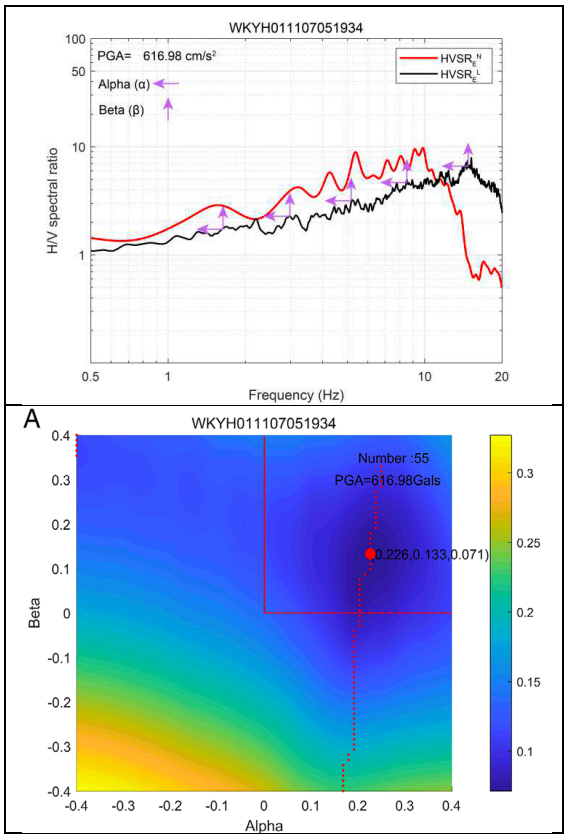

Figure 7: Principle of determination of α and β parameters by comparison of $HVSR_E^{NL}(f)$ and $HVSR_E^{L}(f)$ curves (From Wang, 2022)

While the initial H/V analysis by Wang et al. (2023) considered all K-NET and KiK-net recordings from 1996 to 2020, and all sites having at least 5 weak motion recordings to constrain the linear H/V ratio, we consider here only a selection of low frequency (62) and high frequency (48) sites performed on the basis of linear f_{0HV} values. Each strong recording (PGA > 100 cm/s^2) has been analyzed to derive the α_{ij} and β_{ij} for each site i and event j we have considered here. For simplicity sake, only the statistics on α and β values for the two site classes have been derived for different PGA bins. The results, displayed in Figure 8 do not exhibit actually any major change between low and high frequency sites, especially on the β parameter, which are mostly positive up to a PGA of 700 cm/s^2 and thus indicate a NL trend to increase the amplification in the considered [5 – 20 Hz] frequency range. Once again this result is definitely at odds with the Grenoble site response displayed in Figure 2.

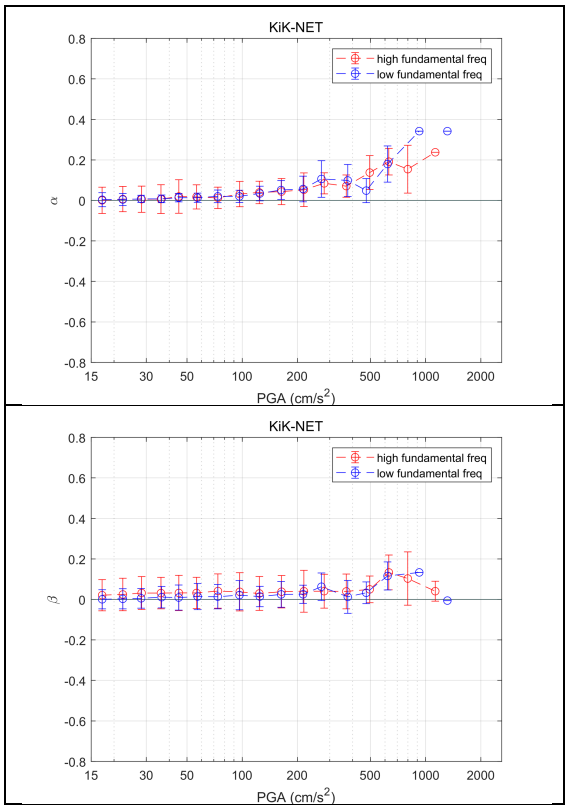

Figure 8: Comparison of α (top) and β (bottom parameters as a function of PGA bin for low (blue) and high(red) f0HV KiKnet recrodings

6 CONCLUSION

From this multi-approach analysis of observed ground motion for large amplitude recordings with rich enough site metadata to analyze the NL modifications as a function of loading parameter AND site characteristics (soft and stiff – V_{S30} value - on one side, and thick and thin – f_{0HV} value – on the other), we did not find any convincing evidence that very soft and/or very thick sites exhibit a peculiar behavior under strong loading. The normalized borehole surface PGA amplifications, the surface to borehole Fourier spectral ratios, and the H/V Fourier spectral ratios, do depict some statistical differences between the thick or soft, and thin or stiff sites. However, such differences are far less pronounced than those predicted by Non-linear / Linear equivalent site response computations for several hundred meters thick sedimentary sites with a large velocity contrast at large depth, such as the Grenoble site.

This analysis would deserve to be extended to a larger set of recordings including the latest very strong Japanese recordings, rather than using only already

databases obtained some years (or decade) ago, and may be a few other approaches to derive the site specific term for each recording and event. This is presently under way. Nevertheless, we also looked at another, more qualitative information: the distribution of site proxies (V_{S30}, f_{0HV}, H_{800} and $Z_{1.5}$) for all Knet and KiKnet sites, and their values for all sites having up to early 2023 experienced a surface PGA exceeding 0.4 g. The results are displayed in Table 4. One can hardly see a differences between the distributions of all sits and the distibution of large acceleration sites. Would there be, as for Grenoble, a strong reduction of HF contents for large levels of ground motion, the site proxy distribution for the large pga sets should be shifted towards higher $V_{S3}0$, f_{0HV}, H_{800} or $Z_{1.5}$ values.

Site proxy	Data set	Number of sites	Average	Standard deviation	Skew	Kurtosis
VS30	All Knet sites	1045	503	255,00	1,93	8,20
	Large pga Knet sites	188	434	268,00	3,03	15,00
	All KiKnet sites	697	500	244,00	1,80	5,80
	Large pga KiK-net sites	113	441	199,00	1,37	2,27
F0HV	All Knet sites	1045	4,12	3,90	1,37	1,67
	Large pga Knet sites	188	4,12	3,81	1,51	2,64
	All KiKnet sites	697	5,57	4,14	0,81	0,45
	Large pga KiK-net sites	113	5,41	3,70	0,61	-0,45
H800	All KiKnet sites	697	40,00	57,40	4,07	22,90
	Large pga KiK-net sites	113	44,10	59,00	3,19	12,80
Z1.5	All KiKnet sites	697	70,80	126,00	5,34	34,60
	Large pga KiK-net sites	113	66,20	74,40	3,05	11,90

Table 4: Compared distribution of average, standard deviation, skew and kurtosis values four site proxies (VS30, f0HV, H800 and Z1.5 from top to bottom) for the whole set of KiKnet and Knet sites, and those which experienced a PGA exceeding 400 cm/s2 between 1996 and early 2023. Knet values are not shown for H800 and Z1.5, since such values are generally not available form the 20 m deep geological and geophysical logs

REFERENCES

1) Ameri, G. & Giannakou, A. (2014). Site response analysis for the Grenoble site and examples of calculation of site GMRS. Technical report GTR/CEA/1014-2017 for Sigma project(WP3), 23 pages + Annex
2) Chandra, J., Gu.guen, P., & Bonilla, L.F., (2016). PGA-PGV/Vs considered as a stress–strain proxy for predicting nonlinear soil response. Soil Dyn. Earthq. Eng. 85, 146–160. https://doi.org/10.1016/j.soildyn.2016.03.020.
3) Darendeli, B.S. (2001). "Development of a New Family of Normalized Modulus Reduction and Material Damping Curves". PhD Dissertation, The University of Texas at Austin, UMI Number:3025211.
4) Deepsoil V5.1 (2012), "User Manual and Tutorial" Youssef M. A. Hashash, Department of Civil and Environmental Engineering,University of Illinois at Urbana-Champaign
5) Derras, B., Bard, P. Y., Régnier, J., & Cadet, H. (2020). Non-linear modulation of site response: Sensitivity to various surface ground-motion intensity measures and site-condition proxies using a neural network approach. Engineering Geology, 269, 105500.
6) Guéguen, P., Bonilla, L.F., & Douglas, J. (2019). Comparison of soil nonlinearity (in situ stress–strain relation and G/Gmax reduction) observed in strong-motion databases and modeled in ground-motion prediction equations. Bull. Seismol. Soc. Am. 109, 178–186. https://doi.org/10.1785/0120180169.
7) Idriss, I. M. (2011). Use of Vs30 to represent local site conditions, in Proceedings of the 4th IASPEI/IAEE International Symposium. Effects of Source Geology on Seismic Motion, August (23–26).
8) Menq, F.Y. (2003). "Dynamic Properties of Sandy and Gravelly Soils". PhD Dissertation, The University of Texas at Austin
9) Pecker, A., Faccioli, E., Gurpinar, A., Martin, C., & Renault, P. (2017). An overview of the SIGMA research project: A European Approach to Seismic Hazard Analysis, *Geotechnical, Geological, and Earthquake Engineering, edited by: Ansal, A*. DOI: 10.1007/978-3-319-58154-5
10) Régnier, J., Bonilla, L. F., Bard, P. Y., Bertrand, E., Hollender, F., Kawase, H., ... & Verrucci, L. (2018). PRENOLIN: International benchmark on 1D nonlinear site-response analysis—Validation phase exercise. Bulletin of the Seismological Society of America, 108(2), 876-900.
11) Régnier, J., Cadet, H., Bonilla, L., Bertand, E., & Semblat, J.F. (2013). Assessing nonlinear behavior of soils in seismic site response: statistical analysis on KiK-net strong-motion data. Bull. Seismol. Soc. Am. 103 (3), 1750–1770. https://doi.org/10.1785/0120120240.
12) Régnier, J., H. Cadet and P.-Y. Bard, 2016. Empirical quantification of the impact of non-linear soil behavior on site response. Bull. Seism. Soc. Am., Vol. 106, No. 4, pp. 1710-1719, doi: 10.1785/0120150199.
13) Wang, Z., Nagashima, F., & Kawase, H. (2021). A new empirical method for obtaining horizontal site amplification factors with soil nonlinearity. Earthquake Engineering & Structural Dynamics, 50(10), 2774-2794.
14) Wang, Z., Sun, J., Ito, E., Kawase, H., & Matsushima, S. (2023). Empirical method for deriving horizontal site amplification factors considering nonlinear soil behaviors based on K-NET and KiK-net records throughout Japan. *Bulletin of Earthquake Engineering*, 1-26.
15) Wang, Z., 2022. Integrated Study on Seismological Site Effects Based on Empirical Methods Considering Linear and Nonlinear Soil Behaviors, PhD dissertation, University of Kyoto, 283 pages
16) Zhu, C., Weatherill, G. Cotton, F., Pilz, M., Kwak, D.Y. & Kawase, H. (2020). An Open-Source Site Database of Strong-Motion Stations in Japan: K-NET and KiK-net. https://doi.org/10.5880/GFZ.2.1.2020.006